J Mater Sci (2009) 44:5563–5568
DOI 10.1007/s10853-009-3779-y

# Synthesis and characterization of $BaTiO_3$-based X9R ceramics

**Ling-xia Li · Ye-mei Han · Ping Zhang · Cui Ming · Xue Wei**

Received: 15 April 2009 / Accepted: 24 July 2009 / Published online: 6 August 2009


**Abstract** The effects of $(Na_{0.5}Bi_{0.5})TiO_3$ (NBT) and MgO addition on the dielectric properties and microstructures of $BaTiO_3$ (BT) ceramics were investigated. NBT was first added to $Nb_2O_5$-doped BT system. As NBT content increases from 0 to 0.2 mol, the Curie temperature of the systems shifts to high temperatures and dielectric constant peak at $T_c$ is suppressed evidently. The variation of capacity ($\Delta C/C_{20\ ^\circ C}$ (%)) of the system at 200 °C decreases with increasing NBT content from 0.1 to 0.2 mol, but that of −55 and 125 °C increases monotonously. The stable temperature characteristics of the dielectric properties improved by NBT doping would be connected with the distortion and deformation of the structure induced by substitution of $Na^+$ and $Bi^{3+}$ into Ba sites. MgO was employed to further flatten the $\Delta C/C_{20\ ^\circ C}$–$T$ curve. It is very helpful for this ceramic system to satisfy the requirement of EIA-X9R specification on $\Delta C/C_{20\ ^\circ C}$ and still keep a satisfied dielectric constant. The addition of MgO improved effectively the temperature stability of the dielectric properties. Changes of the crystalline structure and microstructure induced by MgO doping might contribute to these improvements.

## Introduction

Since the discovery of the high dielectric properties of $BaTiO_3$ ceramics, many investigators have tried to modify this compound in order to achieve stable capacitors with satisfactory operational capacity. Many $BaTiO_3$-based X7R multilayer ceramic capacitors (MLCCs) have been widely used for miniaturization of electronic components attributed to their temperature-stable dielectric behavior ($\Delta C/C_{20\ ^\circ C}$ less than ±15%) over the temperature range from −55 to 125 °C [1–4]. Subsequently, MLCCs have been used under very harsh conditions, such as in the engine electronic control unit (ECU), anti-lock brake system (ABS), and the modules are subjected to high temperature approximately above 130 °C when working in an engine room. Some ceramic systems based on $BaTiO_3$ satisfying the X8R specification (TCC ≤ ±15% from −55 to 150 °C) have also been developed [5–7]. In recent years, MLCCs, which only satisfy the X8R specification, are not good enough to be employed for electronic devices subjected to temperature higher than 150 °C. Therefore, attention should be given to the EIA-X9R specification, in which the variation of capacity is within ±15% of room temperature capacitance in the range of −55 to 200 °C. Owning to its excellent performance for making X7R and X8R ceramics, $BaTiO_3$ ceramics is preferred for X9R ceramics synthesis. However, it is difficult for $BaTiO_3$ to satisfy the X9R specification. As it is well known, $BaTiO_3$ has a tetragonal structure at room temperature and changes to a cubic structure on heating. The temperature of the phase transition from tetragonal to cubic is called Curie temperature ($T_c$). When $BaTiO_3$ is heated over the $T_C$, it undergoes a phase transformation from ferroelectric state to a paraelectric state, which is accompanied by a sharp variation of capacitance. Therefore, many additives have been added to $BaTiO_3$ to modify the temperature–capacitance characteristics. It has been proposed to shift the Curie point to higher temperatures by replacing Ba sites with smaller ionic radius elements to improve the temperature

L. Li (✉) · Y. Han · P. Zhang · C. Ming
School of Electronic and Information Engineering, Tianjin University, 300072 Tianjin, People's Republic of China
e-mail: lilingxia@tju.edu.cn

X. Wei
The Second Resthouse of Tianjin Administrative Affaires, 300072 Tianjin, People's Republic of China

stability of ceramics consisting $BaTiO_3$ as the main component [8].

$(Na_{0.5}Bi_{0.5})TiO_3$ (NBT) is an attractive ferroelectric material, which has strong ferroelectricity at room temperature and relatively high Curie temperature, $T_c = 320$ °C [9]. NBT is considered to be a suitable material to improve the electrical properties of $BaTiO_3$-based ceramics [10–13]. In this article, $Nb_2O_5$-doped $(1 - x)BaTiO_3$–$x(Na_{0.5}Bi_{0.5})TiO_3$ solid solution have been synthesized. MgO additive was employed to further enhance the temperature stability of dielectric properties to meet for EIA-X9R specification and structural and dielectric properties of the BT-based X9R ceramics were characterized and analyzed.

## Experimental

### Sample preparation

$BaTiO_3$ and NBT powders were individually synthesized by conventional solid-state method from reagent-grade oxide powders: $BaCO_3$, $TiO_2$ and $Na_2CO_3$, $Bi_2O_3$, $TiO_2$, respectively. The raw materials were mixed according to the chemical formula by ball milling. The mixtures were dried and calcined at 900 and 1,000 °C for 2 h, respectively. Powders of BT, $Nb_2O_5$ and different amount of NBT were mixed in deionized water by ball milling and then calcined at 900 °C for 2 h. After calcinations, MgO was added and the mixture was ball-milled for 24 h, dried and granulated with PVA as a binder. Then the granulated powders were pressed into disks and the disks were sintered at 1,150 °C for 2 h in air.

### Measurements

X-ray diffraction (XRD) analyses were carried out for phase identification with Cu $K_\alpha$ radiation. The surface microstructure of sintered ceramics was observed with scanning electronic microscope (SEM). The chemical composition analyses of the samples were conducted with an energy dispersive spectrometer (EDS). After samples were fired at 800 °C with silver paste on both sides, dielectric measurements of the samples were performed by using LCR meter (HP4278A) at 1 Hz in the temperature range from −55 to 200 °C. The dielectric constant ($\varepsilon_r$) and the variation of capacity ($\Delta C/C_{20\ ^\circ C}$ (%)) were calculated from the measured capacitance. Insulation resistance was measured using a high resistance meter (Super-High Resistance Meter Model ZC36) at room temperature.

## Results and discussions

### Effect of NBT content on $Nb_2O_5$-doped $(1 - x)BaTiO_3$–$x(Na_{0.5}Bi_{0.5})TiO_3$ systems (abbreviated as $(1 - x)$BT–$x$NBT systems)

The XRD patterns of $(1 - x)$BT–$x$NBT ($x = 0$, 0.1, 0.15, 0.2) sintered at 1,150 °C in Fig. 1 show a clear perovskite phase. It indicates that all the $(1 - x)$BT–$x$NBT ceramics were perovskite structure and the crystal structure was influenced by NBT addition. As it can be seen, diffraction peaks shift gradually toward high degree with increasing NBT content, indicating that interplanar distance decreases. XRD revealed that the crystal structure was influenced by NBT addition. This can be explained by distortion and deformation of the structure, which took place when $Bi^{3+}$ and $Na^+$ ions were substituted into Ba sites, because the ionic radii of $Bi^{3+}$ and $Na^+$ are smaller than that of $Ba^{2+}$. It should also be noted that the diffraction peaks of systems split, which means the substitution into Ba sites induce deformation and distortion of crystal lattice structure. These characteristics indicate a gradual change in crystalline structure and microstructure with NBT concentration.

Dielectric properties of $(1 - x)$BT–$x$NBT as a function of the NBT content are summarized in Table 1. All the ceramics have relatively low dielectric loss, tan$\delta$. The value increases with increasing NBT content from 0.1 to 0.2 mol and the minimum value of the dielectric loss was obtained with 0.1 mol NBT addition. The insulation resistance of the systems was also enhanced noticeably by NBT doping, the overall insulation resistance NBT-doped ceramics were higher than $10^{13}$ Ω cm comparing with $6.5 \times 10^{12}$ Ω cm of undoped BT ceramics.

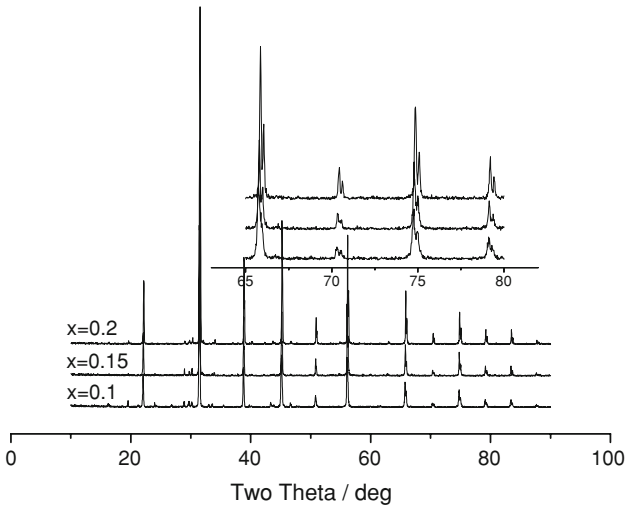


**Fig. 1** X-ray diffraction patterns of $(1 - x)$BT–$x$NBT ($x = 0.1$, 0.15, 0.2) systems

**Table 1** Dielectric properties of $(1 - x)$BT–$x$NBT samples

| $x$ (mol) | Dielectric constant ($\varepsilon_r$) | Temperature coefficient of capacitance ($\Delta C/C_{20\ ^\circ C}$ (%)) | | | Dielectric loss (tan$\delta$) | Insulation resistance ($\rho_v$ $10^{12}$ Ω cm) |
|---|---|---|---|---|---|---|
| | | −55 °C (%) | 125 °C (%) | 200 °C (%) | | |
| 0 | 2,456 | −16.28 | 27.27 | −39.85 | 0.0153 | 6.5 |
| 0.1 | 1,292 | −11.81 | 10.20 | −25.10 | 0.014 | 27.8 |
| 0.15 | 1,294 | −22.63 | 27.09 | −17.42 | 0.0198 | 19.5 |
| 0.2 | 1,111 | −26.25 | 30.32 | −4.98 | 0.022 | 57.6 |

Variation of capacity, $\Delta C/C_{20\ ^\circ C}$ (%), changes with NBT content evidently. As it can be seen in Table 1, addition of 0.1 mol NBT effectively improved $\Delta C/C_{20\ ^\circ C}$ (%) at −55 and 150 °C, and variation of capacity is within ±15% in the range of −55 to 150 °C; when the NBT content increased from 0.1 to 0.2 mol, $(\Delta C/C_{20\ ^\circ C})_{-55\ ^\circ C}$ and $(\Delta C/C_{20^\circ C})_{150\ ^\circ C}$ increase significantly. $\Delta C/C_{20\ ^\circ C}$ of 200 °C decreased gradually with NBT content increasing from 0.1 to 0.2 mol. This indicates that addition of NBT to the system effectively improve temperature stability of capacitance at high temperature. The improvement was attributed to a combination of Curie temperature ($T_C$) shifting with NBT content and lattice distortion induced by substitution of $Ba^{2+}$ by $Na^+$ and $Bi^{3+}$.

It can be evidently seen that the dielectric constant of the ceramics was also affected to a large extent by NBT addition. Room temperature dielectric constant decreases obviously from 2,456 for BT ceramics to 1,292 for 0.1 mol NBT-doped ceramics. As the NBT content increased from 0.1 to 0.2 mol, room temperature dielectric constant decreased gradually. This is because that the pure NBT has low permittivity and structure lattice distortion induced by the substitution, which decreases polarization of the ceramics. The temperature dependence of the dielectric constant with the NBT content is summarized in Fig. 2.

Figure 2 shows the temperature dependence of the dielectric constant, $\varepsilon_r$, of the ceramics as a function of NBT content. It is found that the overall dielectric constant was decreased evidently by doping with NBT. Curie temperature [14], $T_c$, of ceramics increases as NBT content increases and $T_c$ attains the maximum value of 140 °C when the addition of NBT is 0.2 mol, which are similar to the result obtained by Lanfang Gao [12]. It was also noticed that incorporation of NBT to BT ceramics effectively depressed the Curie peaks compared with comparatively obvious Curie peaks of undoped one. Besides, the shape of the $\varepsilon_r$–$T$ curves near the Curie point becomes broad with increasing NBT content. The origin of such behavior might be in connection with the substitution of $Ba^{2+}$ by $Na^+$ and $Bi^{3+}$ to the perovskite cell. As both the ionic radii of $Na^+$ and $Bi^{3+}$ are smaller than that of $Ba^{2+}$, this substitution to Ba sites of perovskite cell would cause distortion of grain lattices, which would change the dipolar

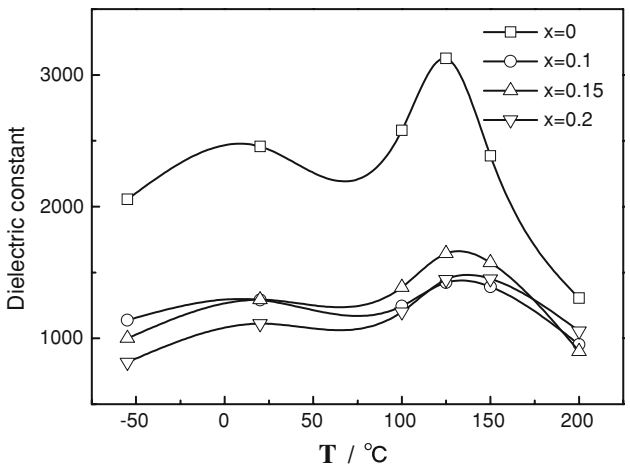


**Fig. 2** Temperature dependence of the dielectric constant for $(1 - x)$BT–$x$NBT ($x = 0$, 0.1, 0.15, 0.2)

moment. In addition, the substitution of $Ba^{2+}$ by $Na^+$ and $Bi^{3+}$ induced the compositional inhomogeneity, which results in the multiphase character over a relatively wide temperature range. The combination of lattice distortion and constituent fluctuations contribute to the improvement of temperature stability of dielectric properties of the system. Therefore, the dielectric peaks were depressed and the curves were flattened over broad temperature range. The shapes of curves differ slightly from previous results [12] because of addition of $Nb_2O_5$.

The optimal dielectric properties are obtained for 0.1 mol NBT-doped ceramics, shown in Table 1, which are: $\varepsilon_r = 1{,}292$, $\tan\delta = 0.014$, $\rho_v = 27.8 \times 10^{12}$ Ω cm, $\Delta C/C_{20}$ is −11.81, 10.20, −25.10% at −55, 150, 200 °C, respectively. It can be concluded that this ceramics have great potential as EIA-X9R-type ceramics.

## Effect of MgO addition on $Nb_2O_5$-doped $0.9BaTiO_3$–$0.1(Na_{0.5}Bi_{0.5})TiO_3$ system (abbreviated as 0.9BT–0.1NBT system)

In order to further enhance the temperature stability of capacitance, MgO was added to 0.9BT–0.1NBT system. Table 2 summarizes the dielectric properties of MgO-doped 0.9BT–0.1NBT ceramics. The overall dielectric

**Table 2** Dielectric properties of MgO-doped 0.9BT–0.1NBT ceramics

| $x$ (mol%) | Dielectric constant ($\varepsilon_r$) | Temperature coefficient of capacitance ($\Delta C/C_{20\ ^\circ C}$ (%)) | | | Dielectric loss (tan$\delta$) | Insulation resistance ($\rho_v$ $10^{12}$ Ω cm) |
|---|---|---|---|---|---|---|
| | | −55 °C (%) | 125 °C (%) | 200 °C (%) | | |
| 0.5 | 1,008 | −10.93 | 26.31 | −20.82 | 0.0150 | 1.73 |
| 1 | 1,000 | −6.3 | 10.1 | −23.13 | 0.0120 | 6.1 |
| 1.5 | 1,100 | −1.8 | 1.8 | −5.69 | 0.0147 | 1.89 |
| 2 | 1,462 | −4.51 | 16.08 | 20.98 | 0.0398 | 0.34 |

constant of MgO-doped systems were higher than 1,000, varies between 1,000 and 1,462. For the samples doped with 0.5, 1, 1.5 mol% MgO, dielectric loss value is less than 15% and the insulation resistance is higher than $10^{12}$ Ω cm. As it can also be seen in Table 2, $\Delta C/C_{20\ ^\circ C}$ of all the samples shows remarkable improvement except that of the ceramic with 0.2 mol% MgO. $\Delta C/C_{20\ ^\circ C}$ (%) of the samples at −55, 150, and 200 °C decrease obviously as MgO content increases from 0.5 to 1 mol%. On the contrary, as MgO content increases up to 2 mol%, insulation resistance decreases, $\Delta C/C_{20\ ^\circ C}$ and dielectric loss increase. These characteristics indicate that addition of proper amount of MgO improves the temperature stability of capacitance noticeably while keep dielectric loss and insulation resistance satisfied. Specially, the 1.5 mol% MgO-doped 0.9BT–0.1NBT ceramics was found to satisfy the EIA-X9R characteristic specification. The dielectric properties are: $\varepsilon_r = 1100$, $\tan\delta = 0.0147$, $\rho_v = 1.89 \times 10^{12}$ Ω cm, $\Delta C/C_{20\ ^\circ C}$ is −1.8, 1.8, and −5.69% at −55, 125, and 200 °C, respectively.

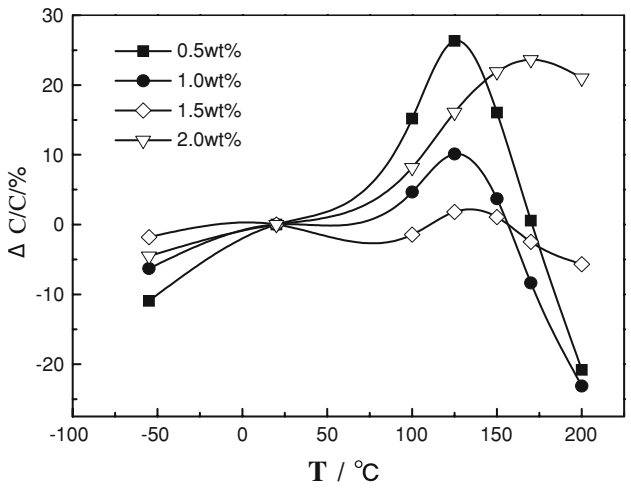


**Fig. 3** $\Delta C/C_{20\ ^\circ C}$–$T$ curves of 0.9BT–0.1NBT ceramics as a function of MgO content

$\Delta C/C_{20\ ^\circ C}$–$T$ curves of 0.9BT–0.1NBT ceramics as a function of MgO content are presented in Fig. 3. It is found that the curves of $\Delta C/C_{20\ ^\circ C}$–$T$ vary obviously with the content of MgO. They reveal that MgO influences significantly on the variation of capacity of the systems. The $\Delta C/C_{20\ ^\circ C}$–$T$ curves were flattened and peaks were broadened noticeably for MgO content $x$ from 0.5 to 1.5. Especially for sample with 1.5 mol% MgO doping, $(\Delta C/C_{20\ ^\circ C})_{-55^\circ C}$ and $(\Delta C/C_{20\ ^\circ C})_{200\ ^\circ C}$ are −1.8 and −5.69%, respectively. Therefore, $0.9BaTiO_3$–$0.1(Na_{0.5}Bi_{0.5})TiO_3$ ceramics with 1.5 mol% MgO exhibited satisfied variation of capacity. Whereas, when $x$ increased up to 2 mol%, the temperature stability of capacitance worsened, $\Delta C/C_{20\ ^\circ C}$ increased obviously at high temperature, $\Delta C/C_{20\ ^\circ C}$ was larger than 20% at 200 °C.

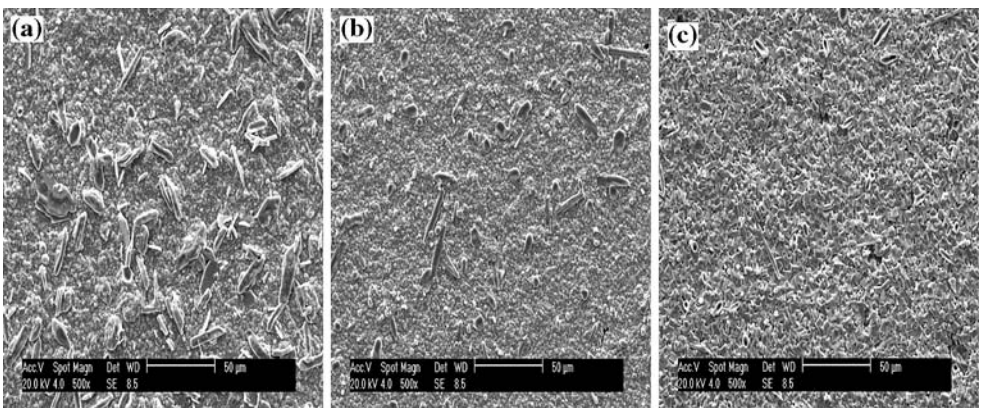


**Fig. 4** SEM micrographs of the ceramics as function of MgO content: **a** $x = 0.5$ mol%; **b** $x = 1.0$ mol%; **c** $x = 2.0$ mol%

These changes might result from that MgO doping, which changed the crystalline structure and microstructure of 0.9BT–0.1NBT ceramics. The diffusion rate of $Mg^{2+}$ into core is low. With small amount of MgO doping, $Mg^{2+}$ does not dissolve deeply into the perovskite cells easily, but rather tends to stay in the grain boundary region of BT, leading to formation of solid solution. The existence of the solid solution in the grain boundaries yields a huge stress, which is considered to be related to temperature stability of capacitance. When too much MgO was added to the ceramics, the inhomogeneous distribution of MgO led to a substantially localized penetration of Mg ions into the core area [15]. This would lead to the change of the crystalline structure, which results in deterioration of temperature stability.

Figure 4 shows the SEM micrographs of the ceramics with different content of MgO. As it is seen in Fig. 4a, there are many pores in grain boundaries and plenty of precipitations on the surface of 0.5 mol% MgO-doped sample. The chemical composition analyses data by SEM–EDS of this sample were shown in Fig. 5. It confirmed that O element and Ti element were main components of the precipitation on the surface. The precipitation decreases with $x$ increasing and merely no precipitation was observed

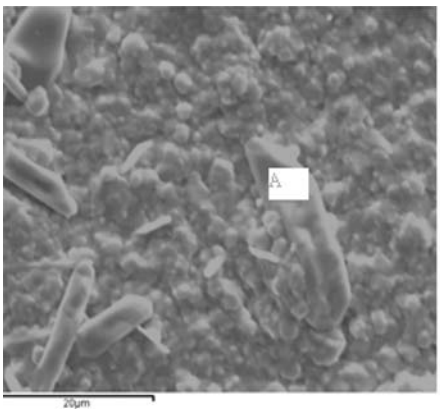

| element | weight percentage (wt. %) | atomic ratio (at. %) |
|---|---|---|
| Mg K | 0.53 | 0.99 |
| Ti K | 28.66 | 27.13 |
| Nb L | 14.72 | 7.18 |
| Ba L | 34.27 | 11.31 |
| O K | 14.64 | 41.50 |

**Fig. 5** SEM–EDS analyses of 0.5 mol% MgO-doped ceramics

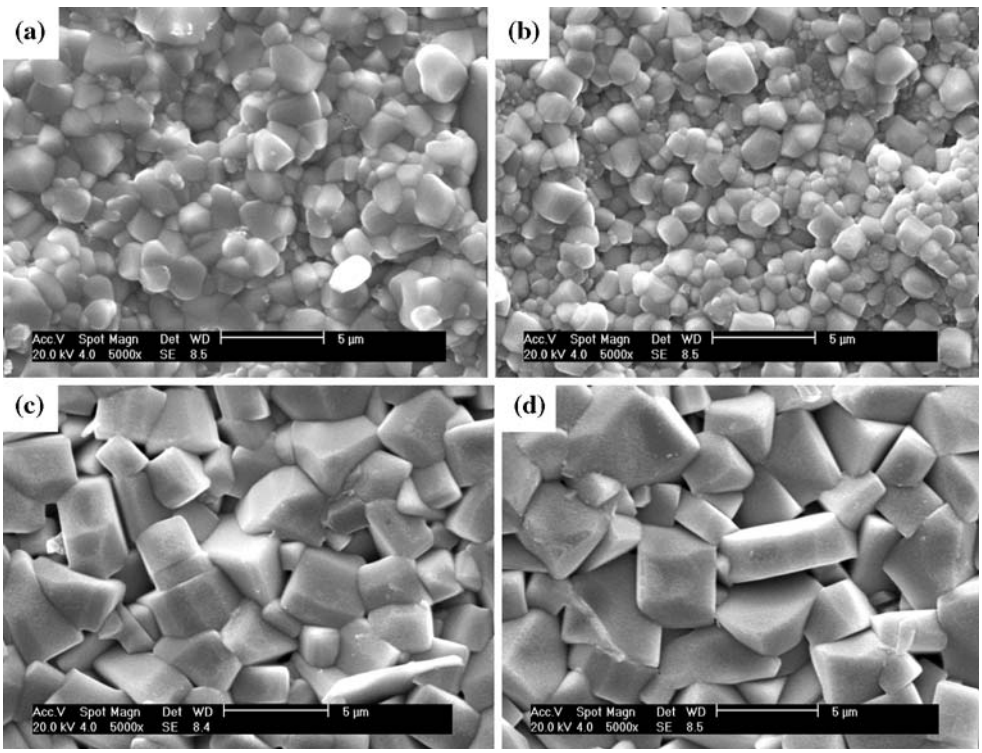


**Fig. 6** SEM photos of ceramics as function of MgO content: **a** $x = 0.5$ mol%; **b** $x = 1.0$ mol%; **c** $x = 1.5$ mol%; **d** $x = 2.0$ mol%

on the surface of ceramics with 2 mol% MgO, which means that the addition of MgO inhibits the elements precipitating effectively.

Figure 6 shows the SEM micrographs of ceramics as a function of MgO content. All these micrographs were taken at the same magnification. From Fig. 6a, b, it can be seen that the sample has agglomeration to certain extent. Fine grains were observed for samples with lower MgO content ($x = 0.5,\ 1.0$). This is because $Mg^{2+}$ ions are probably segregating at grain boundaries, which would inhibit the grain growth [16]. However, there is remarkable grain growth after 1.5 mol% MgO doping and clear grain boundary forms. When $x$ increased to 2.0, grains of the sample (Fig. 6d) grew exaggeratedly, which resulted in abnormal increase in permittivity and deterioration of dielectric loss and temperature coefficient of capacitance, exhibited in Table 2. These changes in microstructures of specimens with MgO content could be responsible for dielectric properties shown in Fig. 3 and Table 2. It can be concluded that MgO addition changes the microstructure of 0.9BT–0.1NBT system and this change leads to the enhancement of dielectric properties, which matches with the rule of X9R ceramics.

## Conclusions

1. $Nb_2O_5$-doped $(1 - x)$BT–$x$NBT ($x = 0, 0.1, 0.15, 0.2$) ceramics has been synthesized by conventional solid-state reaction method. Dielectric properties of BT ceramics was affected noticeably by NBT doping. NBT content influences significantly on the variation of capacity. The improvement of temperature stability of capacitance was attributed to the lattices distortion and structure deformation induced by substitution of $Na^+$ and $Bi^{3+}$ into Ba sites.
2. MgO was employed to further enhance the capacitance temperature stability to match the rule of X9R ceramics. Addition of proper amount of MgO improves the temperature stability of capacitance effectively while it keeps other dielectric parameters satisfied. $\Delta C/C_{20\ ^\circ C}$ of the ceramics was improved with MgO content from 0.5 to 1.5 mol%, but worsened when $x$ increased up to 2 mol%.
3. 1.5 mol% MgO-doped 0.9BT–0.1NBT ceramics was found to satisfy the EIA-X9R characteristic specification. The dielectric properties are: $\varepsilon_r = 1{,}100$, $\tan\delta = 0.0147$, $\rho_v = 1.89 \times 10^{12}\ \Omega$ cm, $\Delta C/C_{20\ ^\circ C}$ is $-1.8$, 1.8, and $-5.69\%$ at $-55$, 125, and 200 °C, respectively.

**Acknowledgements** This work was supported by Program for New Century Excellent Talents in University (NCET) and 863 program (2007AA03Z423) and China Postdoctoral Science Foundation.

## References

1. Li Q, Qi JQ et al (2001) J Eur Ceram Soc 21:2217
2. Li B, Zhang SR et al (2007) J Mater Sci 42:5223. doi: 10.1007/s10853-006-0604-8
3. Chen RZ, Wang XH, Gui ZL, Li LT (2003) J Am Ceram Soc 86:1022
4. Chen RZ, Wang XH, Li LT, Gui ZL (2003) Mater Sci Eng B 99:298
5. Wang S, Zhang SR et al (2006) Mater Lett 60:909
6. Wang S, Zhang SR et al (2006) J Mater Sci 41:1813. doi: 10.1007/s10853-006-2951-x
7. Song YH, Hwang JH, Han YH (2005) Jpn J Appl Phys 44:1310
8. Jung YS, Na ES, Paik U, Lee J, Kim J (2002) Mater Res Bull 37:1633
9. Smolenskii GA, Isupo VA, Agranovskaya AI (1961) Sov Phys Solid State 2:2651
10. Takenaka T, Maruyama K, Sakata K (1991) Jpn J Appl Phys 30:2239
11. Suchanicz J, Kusz J, Böhm H (2003) Mater Sci Eng B 97:154
12. Gao LF, Huang YQ et al (2007) Ceram Int 33:1041
13. Takeda H, Aoto W, Shiosaki T (2005) Appl Phys Lett 87:102104
14. Suchanicz J, Kusz J et al (2003) J Eur Ceram Soc 23:1559
15. Park JS, Han YH (2007) J Eur Ceram Soc 27:1077
16. Kishi H, Kohzu N et al (1999) J Eur Ceram Soc 19:1043